Journal of Power Sources 375 (2018) 345–350

Contents lists available at ScienceDirect

Journal of Power Sources

journal homepage: www.elsevier.com/locate/jpowsour

Electrocatalytic oxidation of meso-erythritol in anion-exchange membrane alkaline fuel cell on PdAg/CNT catalyst

Neeva Benipal [a], Ji Qi [b, 1], Ryan F. McSweeney [a], Changhai Liang [b], Wenzhen Li [a, c, *]

[a] Department of Chemical and Biological Engineering, Biorenewables Research Laboratory, Iowa State University, Ames, IA 50011, USA
[b] School of Chemical Engineering, Dalian University of Technology, Dalian 116024, China
[c] Ames Laboratory, USDOE, Ames, IA 50011, USA

HIGHLIGHTS

- PdAg/CNT (<3 nm average crystallite size) is used for meso-erythritol oxidation.
- PdAg/CNT exhibits high power density in direct meso-erythritol fuel cells.
- Electro-oxidation activity of meso-erythritol intermediates are conducted.
- Pathway for meso-erythritol electro-oxidation on PdAg/CNT at high pH is proposed.
- A preliminary mechanism of meso-erythritol C-C cleavage is provided.

GRAPHICAL ABSTRACT

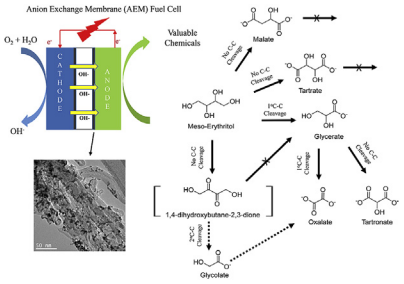

ARTICLE INFO

Article history:
Received 1 May 2017
Received in revised form
24 June 2017
Accepted 27 June 2017
Available online 6 July 2017

Keywords:
Biomass renewables
Meso-erythritol oxidation
Anion-exchange membrane fuel cell
PdAg nanoparticles
Electrocatalysis

ABSTRACT

C-C bond cleavage during electrocatalytic oxidation of glycerol and C_{3+} polyols often occurs and can significantly affect the Faradaic efficiency, fuel utilization, and output power density of a direct polyol fuel cell, although this has not been deeply investigated. With the goal of acquiring new knowledge of C-C bond breaking of polyols, this study examines the electrocatalytic oxidation of a C_4 polyol meso-erythritol on carbon nanotube supported Pd-based catalysts (Pd/CNT, PdAg/CNT, and $PdAg_3$/CNT) in an anion-exchange membrane fuel cell (AEMFC). Our results show that PdAg/CNT improves the fuel efficiency of meso-erythritol oxidation by contributing to the C-C bond cleavage of meso-erythritol in C_3 and C_2 chemicals. Based on the analysis of electro-oxidation products and half-cell cyclic voltammetry (CV) of intermediates, a meso-erythritol electro-oxidation pathway has been proposed to demonstrate that Ag is likely to assist Pd to promote the cleavage of C-C bonds of meso-erythritol.

There is an increasing need to explore environmentally beneficial green energy sources to meet rapidly growing global energy needs resulting from diminishing fossil fuel resources. Sustainable energy conversion and storage technologies, such as fuel cells, metal-air batteries, flow cells, etc., have attracted enormous attention because of both their potential for high energy-conversion efficiency and their environmental advantages [1–5]. Electrocatalysis is anticipated to play an increasingly critical role because it is a promising emerging technology for use in

* Corresponding author. Department of Chemical and Biological Engineering, Biorenewables Research Laboratory, Iowa State University, Ames, IA 50011, USA.
E-mail address: wzli@iastate.edu (W. Li).
[1] Previous address: Department of Chemical and Biological Engineering, Biorenewables Research Laboratory, Iowa State University, Ames, IA 50011, USA.

http://dx.doi.org/10.1016/j.jpowsour.2017.06.082
0378-7753/

biorenewable feedstock conversion for cogeneration of electricity and chemicals via anion exchange membrane fuel cells (AEMFCs) devices [6–9]. AEMFCs have attracted enormous attention by representing a potential solution for alleviating current energy issues [10–13]. In high pH media, the reaction kinetics of alcohol oxidation in the anode and oxygen reduction reactions at the cathode are greatly improved due to facilitated charge transfer.

Polyols (e.g. glycerol, xylitol, sorbitol) have been identified by the U.S-Department of Energy as among the top 10 biomass-derived chemicals and they will serve as feedstock building blocks for future production of chemicals, fuels, and polymers [14,15]. Many research studies have been devoted to the development of highly-selective catalysts for efficiently converting glycerol to higher-valued oxygenated chemicals [8,16–20]. In contrast to Pt and Au catalysts, Pd nanoparticles have demonstrated a unique catalytic ability in enhancing selectivities and achieving deeper C-C cleavage. Electrochemical behavior of C_3 model molecule glycerol on PdAg/CNT anode catalysts in AEMFCs has been thoroughly investigated in our previous studies [21]. That work focused on PdAg/CNT catalyzed alcohol (methanol, ethanol, ethylene glycol, and glycerol) oxidation reactions facilitated by Ag-catalyzed aldehyde oxidation in a general catalytic mechanism [21]. Our more recent work, focused on a more detailed analysis of glycerol oxidation over PdAg/CNT in AEMFCs [22], has shown that the selectivity of C-C bond cleavage products: the C_2 species, i.e., oxalate and glycolate on Pd/CNT, PdAg/CNT, and $PdAg_3$/CNT increased as the Ag content increased, indicating that Ag contributed to deeper oxidation of C-C bond cleavage.

However, deeper insights into C-C cleavage of polyols during electrochemical oxidation have not been achieved. This work attempts to achieve a clearer understanding of C-C cleavage mechanisms and to investigate the simplest polyol with two kinds of C-C bonds, to gain insights into preferable C-C breaking sequence of polyols and lay a necessary foundation for further study of electrocatalytic oxidation of longer carbon chain bio-polyols such as C_5 xylitol or C_6 sorbitol. In contrast to C_3 polyol glycerol that has two identical primary C-C bonds, C_4 polyol meso-erythritol has two primary and two secondary C-C bonds, so this study might provide us with new knowledge with respect to determining which C-C bond is preferably broken. Study of electrocatalytic oxidation of meso-erythritol in alkaline AEMFCs on Pd-based catalysts has not been previously done to the best of our knowledge.

Meso-erythritol (1,2,3,4-butanetetrol) is a sugar polyol used as a food additive because of its health properties, e.g., it is low in calories, is a tooth-friendly sweetener, and is safe for use by diabetics because it has no impact on blood insulin or glucose levels [23,24]. Erythritol is a naturally-occurring molecule found in fruits such as melons, grapes, pears, and in some fermented foods. It has been mass-produced at industrial level from starch, sucrose, glucose via enzymatic, and fermentation processes [25,26]. In addition to its possible applications in polymers, chemistry, and pharmaceuticals, meso-erythritol has also become an interesting subject for possible use in electrochemistry. Cherqaoui et al. demonstrated that meso-erythritol provides a slow reaction with a bare polycrystalline Pt electrode in 0.1 M $HClO_4$ for electrocatalytic oxidation of meso-erythritol, and Fourier transform infrared spectroscopy (FTIR) was used to study reaction mechanisms for the oxidation of erythritol [27]. Meso-erythritol has also received some attention in the electrochemistry area. Electrocatalytic studies of oxidation of meso-erythritol appear to hold great promise for future development of alkaline AEMFCs in cogeneration of higher-valued chemicals and electrical energy, and its detailed reaction pathway need to be elucidated.

In this communication, Pd, Ag mono, and bimetallic nanoparticles supported on carbon nanotubes were used for the first time to produce meso-erythritol oxidation in alkaline AEMFCs. The reaction pathways of electrocatalytic oxidation of meso-erythritol into valuable chemicals under mild reaction conditions have been discussed in terms of both half-cell and single-cell findings. The addition of Ag content into Pd catalyst has been found to facilitate C-C bond cleavage of meso-erythritol.

Pd, Ag mono, and bimetallic nanoparticles, supported on carbon nanotubes with particle sizes: 2.0 nm for Pd/CNT, 2.3 nm for PdAg/CNT, 2.4 nm for $PdAg_3$/CNT, and 13.9 nm for Ag/CNT, were prepared using an aqueous-phase reduction method recently developed by our group [8,10,11,21]. The prepared catalysts were comprehensively characterized via X-ray diffraction (XRD), transmission electron microscopy (TEM), X-ray photoelectron spectroscopy (XPS), inductively coupled-plasma-mass spectrometry (ICP-MS), and high-angle annular dark field via aberration-corrected scanning transmission electron microscopy (HAADF-STEM) in our previous publication [22]. As the TEM images shown in Fig. 1a–d, the particle size of Ag nanoparticle can be greatly reduced by alloying with Pd. All the well-dispersed Pd-based nanoparticles were uniformly deposited on the CNT supports. XRD patterns of all catalysts exhibited typical a face-centered cubic (FCC), as seen in Fig. 1e–f. The diffraction peaks of the alloyed PdAg and $PdAg_3$ bimetallic nanoparticles fall between those of monometallic Ag and Pd, suggesting the formation of alloy structure and no obvious phase separation. The similar particle sizes and size distributions of Pd-based catalysts provide a good platform for investigating selective electrooxidation of meso-erythritol in alkaline electrolyte. The aqueous-phase reduction method achieved very small Pd nanoparticles under these synthesis conditions, while the Pd-Ag containing particles were slightly larger. The surface oxidation states of the metals in as-prepared catalysts were characterized by the XPS, as seen in Fig. 1g–h. XPS spectra of monometallic Pd/CNT revealed both oxidized Pd^{2+} and metallic Pd^0 chemical oxidation states. Metallic Ag^0 was primarily present in Ag 3d of Ag/CNT, PdAg/CNT, and $PdAg_3$/CNT catalysts. The addition of Ag to Pd prevents the oxidation of Pd via alloy formation, so in alloyed PdAg/CNT and $PdAg_3$/CNT the existence of only metallic Pd^0 in the surface oxidation state was observed. Pd^0 and Pd^{2+} and Ag^0 were detected, reflecting the efficient reduction of $Pd(NO_3)_2 2H_2O$ and $AgNO_3$. A greater amount of metallic Pd^0 in PdAg/CNT than in monometallic Pd/CNT might enhance the alcohol deprotonation effect, resulting in higher meso-erythritol oxidation kinetics.

Cyclic Voltammetry results show that Pd and Ag, alloyed together (PdAg/CNT or $PdAg_3$/CNT), produced higher current density and lower onset potential than monometallic Pd/CNT and Ag/CNT catalysts, as shown in Fig. 2a. The Ag/CNT material, however, exhibited no activity toward electrocatalytic meso-erythritol oxidation at the same applied potential, leading to the conclusion that Ag is relatively catalytically inactive with respect to alcohol oxidation within fuel cell anode potential (−0.2 V vs. MMO).

The electrocatalytic properties of Pd/CNT, PdAg/CNT, and $PdAg_3$/CNT anode catalysts towards meso-erythritol were then evaluated in AEMFCs under optimized conditions, as shown in Fig. 2b. The open circuit voltage (OCV) of the direct meso-erythritol AEMFC with PdAg/CNT was 0.87 V, 0.14 V higher than for $PdAg_3$/CNT and 0.02 V higher than for Pd/CNT. The peak power density (PPD) of the direct meso-erythritol AEMFC with PdAg/CNT was 153.7 mW cm^{-2}, 17.8% higher than for $PdAg_3$/CNT and 34.5% higher than that for Pd/CNT. The higher content of Ag in $PdAg_3$/CNT catalyst caused the active sites of the Pd catalyst to be covered by Ag, limiting the reaction rate in the higher current density region and decreasing performance.

Meso-erythritol oxidation products were also examined by HPLC on Pd/CNT, PdAg/CNT, and $PdAg_3$/CNT anode catalysts for 2 h at 60 °C in AEMFC at a constant fuel cell voltage of 0.1 V,

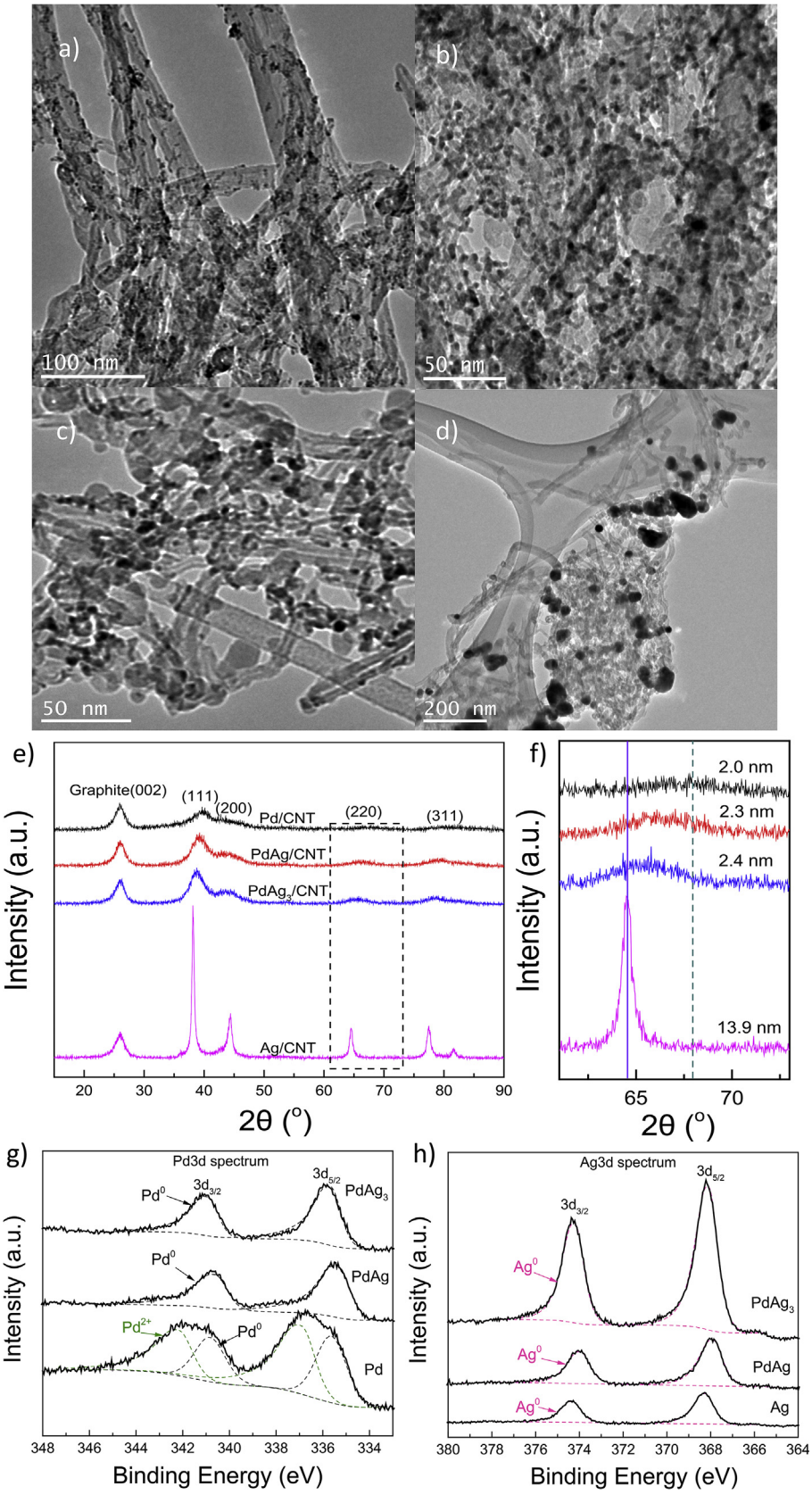

Fig. 1. TEM images of a) Pd/CNT, b) PdAg/CNT, c) $PdAg_3$/CNT, and d) Ag/CNT catalysts; XRD patterns e) with corresponding zoomed 220 peaks f); XPS spectra g) and h) of all these four catalysts.

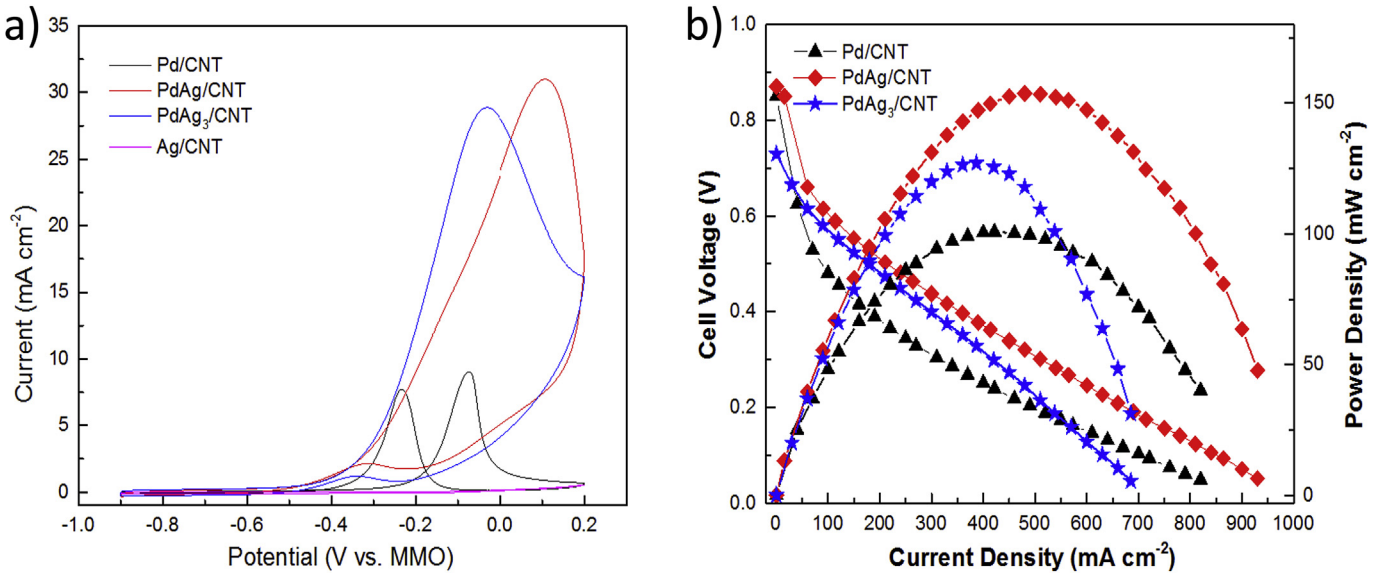

Fig. 2. a) Cyclic voltammograms of Pd/CNT, PdAg/CNT, $PdAg_3$/CNT, and Ag/CNT for meso-erythritol oxidation in N_2 purged 1.0 M KOH +0.1 M meso-erythritol, 50 mV s^{-1}, 25 °C; b) Polarization and power density curves of direct meso-erythritol AEMFC with different anode catalysts (Pd/CNT, 0.5 mg cm^{-2}; PdAg/CNT, 1.0 mg cm^{-2}; $PdAg_3$/CNT, 2.0 mg cm^{-2}). AEM: Tokuyama A201; cathode catalyst: Fe-based catalyst (Acta 4020), 3.0 mg cm^{-2}; anode fuel: 6.0 M KOH + 1.0 M meso-erythritol, 2.0 mL min^{-1}, cathode fuel: O_2, 200 sccm, ambient pressure, 80 °C.

demonstrating selectivities are highly-dependent on the applied potentials [18,28]. It has demonstrated that production of valued chemicals from polyol can be achieved with electricity cogeneration [6]. Table 1 shows the product selectivity distribution of meso-erythritol oxidation; it can be observed that the selectivity of the C_2 species, i.e., oxalate, increased as the Ag content increased, indicating that Ag contributed to a deeper C-C bond cleavage, but the selectivity of C_2 species, i.e., glycolate, decreased as the Ag content increased. The variation in selectivities of the C_2 species must be dependent on whether the C-C bond cleavage occurs on the 1° or 2° carbons of meso-erythritol, as discussed later in the description of the proposed mechanism. Conversely, all the C_3 species and C_4 species, i.e., tartrate, malate, tartronate, and glycerate on Pd/CNT, PdAg/CNT, $PdAg_3$/CNT, decreased as the Ag content increased.

The conversion of meso-erythritol over 2 h interval was 69.4%, 66.4%, and 58.8% for Pd/CNT, PdAg/CNT, $PdAg_3$/CNT, respectively. The increase in Ag content resulted in higher Faradaic efficiencies of 40.3% for Pd/CNT, 41.9% for PdAg/CNT, and 44.7% for $PdAg_3$/CNT, while the fuel utilization efficiency exhibited a decrease in additional of Ag as shown in Table 2. A higher Ag content in a Pd catalyst (in this case Pd_1Ag_3) may block the active sites of Pd and result in a decrease in conversion of $PdAg_3$/CNT, leading to a drop-in fuel utilization efficiency. The fuel utilization is determined by both conversion and Faradaic efficiency. The addition of Ag leads to a trade off between conversion decrease and Faradaic efficiency increase. So that the fuel utilization of Pd/CNT and PdAg/CNT are close to each other. However, further addition of Ag will result in significant conversion drop, which becomes the dominant factor contributing to the apparent fuel utilization drop. At the same time, the carbon balance increased from 82.4% to 93.7%, indicating that fewer C_2 products (glycolate and oxalate) were oxidized into C_1 products (formate and carbonate). The addition of Ag to Pd not only improves the Faradaic efficiency by 9.8%, but also enhances the peak power density by 34.6%.

Table 1
Product selectivity distribution of electrocatalytic oxidation of meso-erythritol on Pd/CNT, PdAg/CNT, and $PdAg_3$/CNT in AEMFC. Anode fuel: 1.0 M KOH+0.5 M meso-erythritol, 2.0 mL min^{-1}, cathode fuel: O_2, 200 sccm, ambient pressure, 60 °C. The numbers below are in %.*1,4-dihydroxybutane-2,3-dione is detected but not quantified; its quantity range can be estimated using carbon balance.

	Oxalate	Tartronate	Tartrate	Malate	Glycerate	Glycolate
Pd/CNT	27.8	10.0	5.0	3.2	25.7	28.4
PdAg/CNT	37.3	7.8	2.5	3.8	22.5	26.1
$PdAg_3$/CNT	49.3	8.1	1.4	3.2	19.9	18.2

The proposed pathway of meso-erythritol oxidation on PdAg/CNT in AEMFC based on oxidation product analysis by HPLC/NMR and CV of important intermediates is shown in Fig. 3. Two stable non C-C breaking C_4 products, tartrate and malate, have been observed. Along with oxidation of two primary hydroxyl groups of meso-erythritol generates tartrate, malate has a similar molecular structure to that of tartrate, and it contains two primary carboxylic acids, one secondary alcohol group, and one secondary methyl group. Malate generation is hypothesized as occurring through coupled heterogeneous electrocatalytic oxidation and homogeneous transformation of meso-erythritol. There is no further oxidization of tartrate and malate based on CV (Fig. S1a and b), suggesting that they are “dead-end products” (No C-C breaking occurred on the two chemicals). Oxidation of two secondary hydroxyl groups of meso-erythritol generates 1,4-dihydroxybutane-2,3-dione with two ketone groups, which is not stable in alkaline electrolyte in nature and could possibly further transform into other products.

On the C-C cleavage mechanism, cleaving one of primary C-C bonds (1° C-C) of an adsorbed C_4 reactive intermediate and then oxidizing the primary hydroxyl group will produce glycerate. Half-cell CV results have shown that two C_4 chemicals in the alkaline electrolyte, tartrate and malate, were stable in the applied potential range. Cleavage of 1,4-dihydroxybutane-2,3-dione's 1° C-C bond will not lead to glycerate production (glyceraldehyde instead is the product, but it is not detected). These results indicate that the three desorbed C_4 chemicals (tartrate, malate, and 1,4-dihydroxybutane-2,3-dione) are not the intermediates, but other C_4 reactive intermediates, which elude from HPLC detection, lead to 1° C-C breakage to produce glycerate.

Glycerate has been shown to be a reaction intermediate during

Table 2
Conversion, carbon balance, average electron transfer, Faradaic efficiency, and fuel utilizations of electrocatalytic oxidation of meso-erythritol on Pd/CNT, PdAg/CNT, and $PdAg_3$/CNT in AEMFC. Anode fuel: 1.0 M KOH +0.5 M meso-erythritol, 2.0 mL min^{-1}, cathode fuel: O_2, 200 sccm, ambient pressure, 60 °C.

	Conversion (%)	Carbon balance (%)	Average electron transfer	Faradaic efficiency (%)	Fuel utilization (%)	Power density (mW cm^{-2})
Pd/CNT	69.4	82.4	7.2	40.3	27.9	100.7
PdAg/CNT	66.4	88.4	7.5	41.9	27.8	153.7
$PdAg_3$/CNT	58.8	93.7	8.0	44.7	26.3	126.3

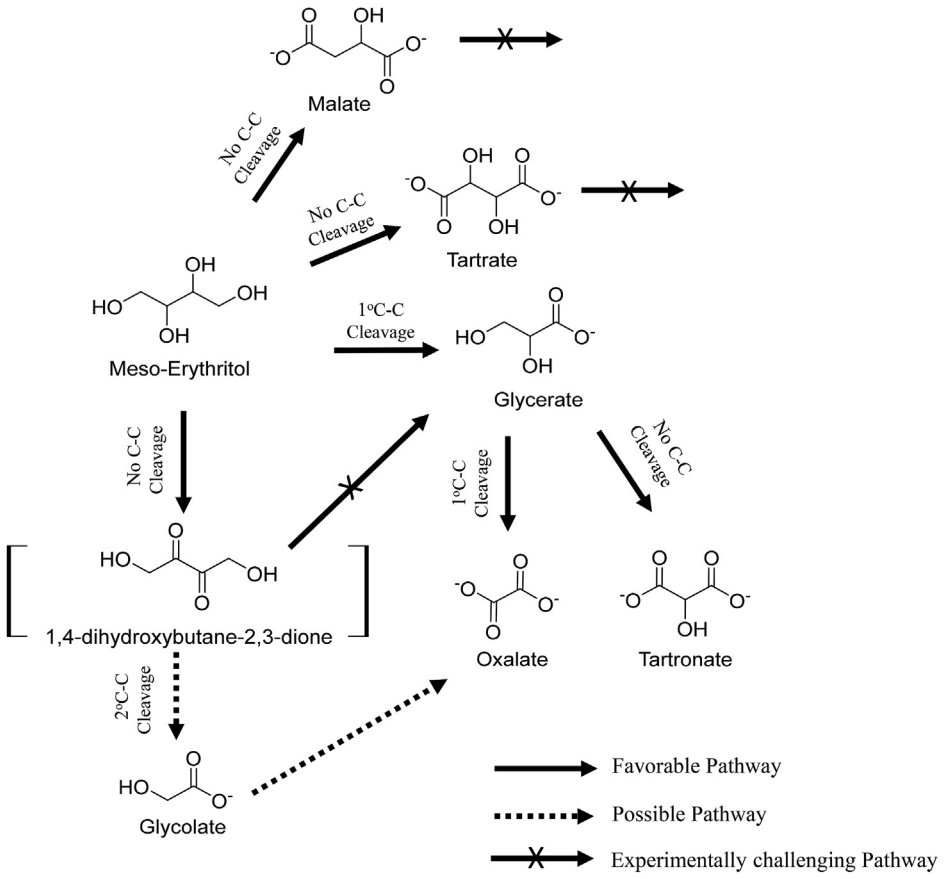

Fig. 3. Proposed reaction pathway for oxidation of meso-erythritol on PdAg/CNT in alkaline media. Notes: These reaction pathways do not necessarily indicate elementary reaction steps. The proposed pathway is based on reaction intermediates/products examined by HPLC/NMR.

the meso-erythritol oxidation reaction on PdAg catalyst (Fig. S2a), and it can be furthermore transformed into C_3 tartronate and C_2 oxalate (a C-C cleavage product) via its electrocatalytic oxidation in AEMFC, as previously reported [22]. In comparison, both tartronate and oxalate were observed to be "dead end products" because their functional groups were not further oxidized (no apparent current generated based on half-cell results), as shown in Fig. S2b and Fig. S3a.

Our experiments show that glycerate oxidation will not lead to glycolate production and that tartronate is a "dead-end product", indicating glycolate is most likely not generated from tartronate and glycerate. We speculate that C_2 chemical glycolate was generated from the *direct secondary C-C bond* (*2° C-C*) *cleavage* of a meso-erythritol-derived C_4 reactive intermediate, in the oxidation process over the PdAg catalyst. In our previous study [21], we found that the C-C bond between a ketone and carboxylic group (O=C-COOH) is easily cleaved within the fuel cell anode potential window, therefore, assuming a C-C bond between two ketone groups (O=C-C=O) can also be cleaved, 1, 4-dihydroxybutane-2,3-dione should be at least one of the reactive intermediates leading to glycolate production via *2° C-C* cleavage of meso-erythritol.

Glycolate in the alkaline electrolyte is known to be an unstable reaction intermediate over PdAg catalysts in the applied potential range (<0.9 V vs. RHE) based on the CVs (Fig. S3b), and we have found that the main product of glycolate oxidation on Pt/C catalyst at 0.6 V vs. RHE is not formate or carbonate (C-C breakage products), but rather oxalate [28]. Therefore, oxalate can be generated from either oxidation of glycolate's hydroxyl group or C-C cleavage of glycerate. As outlined in the reaction pathway (Fig. 3), it is self-evident that glycolate is the only product from 2° C-C breakage of meso-erythritol (likely via the intermediate 1,4-dihydroxybutane-2,3-dione), while glycerate and tartronate are products from 1° C-C breakage of meso-erythritol (derived intermediates). However, since oxalate can be produced from either 1° C-C (oxidation of primary OH in glycolate) or 2° C-C (C-C breakage of glycerate) breakage of meso-erythritol, further study is needed to clarify the ratio of oxalate from glycolate and glycerate and examine the products from 1,4-dihydroxybutane-2,3-dione oxidation, and allow the ratio of 1° C-C cleavage and 2° C-C cleavage to be estimated. This strategy and generated knowledge may be applied to longer

carbon-chain xylitol and sorbitol (C_5, C_6 polyol) electrocatalytic oxidation study.

In conclusion, we have successfully demonstrated cogeneration of electricity and chemicals from electrocatalytic oxidation of meso-erythritol on carbon nanotube supported PdAg catalysts in AEMFCs. The investigation reveals a proposed reaction pathway based on PdAg/CNT under mild conditions while differentiating the C-C bond cleavage on both primary and secondary C-C bonds of meso-erythritol.

Acknowledgements

We acknowledge financial support from the US National Science Foundation (CBET-1159448, 1501124), the Ames Lab startup fund, the Iowa State University startup fund and an Iowa Energy Center (IEC) Opportunity Grant (4781742). We thank Dr. Dapeng Jing of Material Analysis and Research Laboratory of ISU for XPS analysis, and Michael Forrester from Dr. Eric W. Cochran's Lab for synthesizing 1,4-dihydroxybutane-2,3-dione due to its commercial unavailability. The authors are grateful to Baitong Chen of Iowa State University for assistance in fuel cell experiments.

Appendix A. Supplementary data

Supplementary data related to this article can be found at http://dx.doi.org/10.1016/j.jpowsour.2017.06.082.

References

[1] E. I. Administration, Electric Power Annual, U.S. Department of energy, 2016.
[2] Y. Chen, M. Bellini, M. Bevilacqua, P. Fornasiero, A. Lavacchi, H.A. Miller, L. Wang, F. Vizza, ChemSusChem 8 (2015) 524–533.
[3] L. An, T.S. Zhao, L. Zeng, X.H. Yan, Int. J. Hydrogen Energy 39 (2014) 2320–2324.
[4] C.L. Bianchi, P. Canton, N. Dimitratos, F. Porta, L. Prati, Catal. Today 102–103 (2005) 203–212.
[5] M. Besson, P. Gallezot, Catal. Today 57 (2000) 127–141.
[6] Z. Zhang, L. Xin, W. Li, Appl. Catal. B Environ. 119–120 (2012) 40–48.
[7] L. Xin, Z. Zhang, Z. Wang, W. Li, ChemCatChem 4 (2012) 1105–1114.
[8] J. Qi, L. Xin, D.J. Chadderdon, Y. Qiu, Y. Jiang, N. Benipal, W. Li, Appl. Catal. B Environ. 154–155 (2014) 360–368.
[9] D.J. Chadderdon, L. Xin, J. Qi, Y. Qiu, P. Krishna, K.L. More, W. Li, Green Chem. 16 (2014) 3778–3786.
[10] N. Benipal, J. Qi, J.C. Gentile, W. Li, Renew. Energy 105 (2017) 647–655.
[11] N. Benipal, J. Qi, P.A. Johnston, J.C. Gentile, R.C. Brown, W. Li, Fuel 85 (2016) 85–93.
[12] C. Bianchini, P.K. Shen, Chem. Rev. 109 (2009) 4183–4206.
[13] A. Caillé, M. Al-Moneef, F.B. de Castro, A. Bundgaard-Jensen, A. Fall, N.F. de Medeiros, World Energy Council, 2007.
[14] T. Werpy, G. Petersen, National Renewable Energy Lab, 2004.
[15] J.J. Bozell, G.R. Petersen, Green Chem. 12 (2010) 539–554.
[16] S. Carrettin, P. McMorn, P. Johnston, K. Griffin, C.J. Kiely, G.A. Attard, Top. Catal. 27 (2004) 131–136.
[17] S. Carrettin, P. McMorn, P. Johnston, K. Griffin, C.J. Kiely, G.J. Hutchings, Phys. Chem. Chem. Phys. 5 (2003) 1329–1336.
[18] Z. Zhang, L. Xin, J. Qi, D.J. Chadderdon, K. Sun, K.M. Warsko, W. Li, Appl. Catal. B Environ. 147 (2014) 871–878.
[19] Z. Zhang, L. Xin, J. Qi, Z. Wang, W. Li, Green Chem. 14 (2012) 2150–2152.
[20] Z. Zhang, L. Xin, J. Qi, D.J. Chadderdon, W. Li, Appl. Catal. B Environ. 136 (2013) 29–39.
[21] J. Qi, N. Benipal, C. Liang, W. Li, Appl. Catal. B Environ. 199 (2016) 494–503.
[22] N. Benipal, J. Qi, Q. Liu, W. Li, Appl. Catal. B Environ. 210 (2017) 121–130.
[23] G.J.M. den Hartog, A.W. Boots, A. Adam-Perrot, F. Brouns, I.W.C.M. Verkooijen, A.R. Weseler, Nutrition 26 (2010) 449–458.
[24] H. Röper, J. Goossens, Starch - Stärke 45 (1993) 400–405.
[25] M.A.Y. Aoki, G.M. Pastore, Y.K. Park, Biotechnol. Lett. 15 (1993) 383–388.
[26] C.L. Hu, E.A. McComb, V.V. Rendig, Arch. Biochem. Biophys. 110 (1965) 350–353.
[27] A. Cherqaoui, D. Takky, K.B. Kokoh, F. Hahn, E.M. Belgsir, J.M. Léger, J. Electroanal. Chem. 464 (1999) 101–109.
[28] L. Xin, Z. Zhang, J. Qi, D. Chadderdon, W. Li, Appl. Catal. B Environ. 125 (2012) 85–94.